LA-UR-01-2677
Approved for public release;
distribution is unlimited.

Title:

SNS MODELING - HIGH VOLTAGE POWER SUPPLY RIPPLE ANALYSIS

Author(s):

Sung-il Kwon
Joseph Bradley
Amy Regan
Yi-Ming Wang
Tony Rohlev

Submitted to:

http://lib-www.lanl.gov/la-pubs/00796099.pdf

Los Alamos National Laboratory, an affirmative action/equal opportunity employer, is operated by the University of California for the U.S. Department of Energy under contract W-7405-ENG-36. By acceptance of this article, the publisher recognizes that the U.S. Government retains a nonexclusive, royalty-free license to publish or reproduce the published form of this contribution, or to allow others to do so, for U.S. Government purposes. Los Alamos National Laboratory requests that the publisher identify this article as work performed under the auspices of the U.S. Department of Energy. Los Alamos National Laboratory strongly supports academic freedom and a researcher's right to publish; as an institution, however, the Laboratory does not endorse the viewpoint of a publication or guarantee its technical correctness.

FORM 836 (10/96)

Los Alamos
National Laboratory

memorandum
SPALLATION NEUTRON SOURCE

To/MS : Distribution
From/MS : Sung-il Kwon, MS H827
Joseph Bradley
Amy Regan
Yi-Ming Wang
Tony Rohlev

Phone/Fax: 667-3044/Fax 665-2818
E-mail : skwon@lanl.gov
Symbol : SNS-2-TN
Date : 22 November 2000

Subject :

SNS MODELING

- HIGH VOLTAGE POWER SUPPLY RIPPLE ANALYSIS

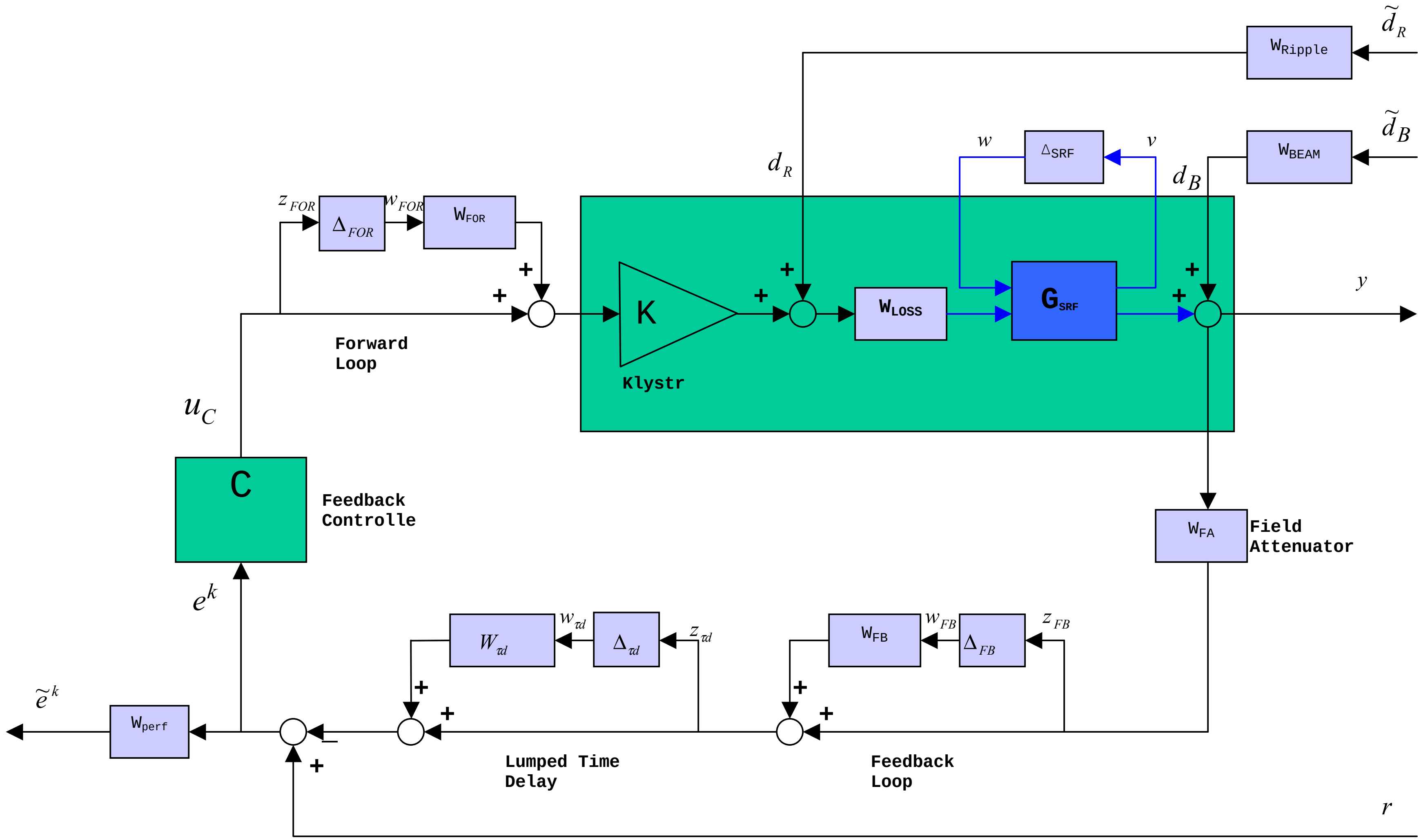

Figure 1 Block Diagram of the perturbed linear accelerator RF system

1. General Description of a Perturbed Closed Loop System

Figure 1 shows the complete model for closed loop system analysis for the low level RF system with a klystron and a cavity.

1. Block K is the klystron.

2. Block P is the cavity; DTL Tank #3, CCL Module #4, and SRF Cavity #90.

3. Block C is the PI feedback controller.

4. Block W_{FA} is the field attenuator that scales the cavity field output to the level of signals in the low level RF system.

5. Block W_{BEAM} is the weighting function for beam current. The beam current is scaled and is represented as the exogenous disturbance, $\tilde{d}_B$.

6. Block W_{Ripple} is the weighting function for high voltage power supply (HVPS) ripple. The HVPS ripple is scaled and is represented as the exogenous disturbance, $\tilde{d}_R$.

7. Feedback loop distortion is the uncertainties in the cavity field feedback loop from cavity to DSP. It is represented by the multiplicative uncertainty.

8. Forward loop distortion is the uncertainties in control signal forward loop from DSP to klystron. It is represented by the multiplicative uncertainty.

9. Lumped time delay is the time delays in the whole loop. The time delays are lumped together and is represented as a multiplicative uncertainty.

10. The performance specification ($\pm 0.5\%$ amplitude error and $\pm 0.5^{\circ}$ phase error in steady state) is represented by the weighting function W_{perf} .

11. The power losses in the transmission (waveguide) is represented by the block W_{LOSS}. When the power losses is x %, then W_{LOSS} becomes

$$W_{LOSS} = \sqrt{(1.0 - \frac{x}{100})} \cdot \begin{bmatrix} 1 & 0 \\ 0 & 1 \end{bmatrix}.$$

12. The cavity parameter perturbations including the Lorentz Force Detuning of SRF cavity is represented by the uncertainty block Δ_{cav} .

Note that multiplicative uncertainty has the form

$$Output = (I + W_{xx} \Delta_{xx}) Input \ .$$

2. Sensitivity Matrix for the High Voltage Power Supply Ripple in the Perturbed Closed Loop System of a SRF Cavity

In order to investigate the effect of the HVPS ripple to the performance, the transfer matrix from the exogenous disturbances $\tilde{d}_R$, $\tilde{d}_B$, and the set point trajectory r to error e^k is obtained with $\Delta_{FB} = 0$, $\Delta_{FOR} = 0$.

$$E^k(s) = R(s) - (I + W_{\tau d}\Delta_{\tau d})W_{FA}Y(s) = R(s) - (I + W_{\tau d}\Delta_{\tau d})W_{FA}\left(W_{BEAM}\tilde{d}_B(s) + P\left(KU_C(s) + W_{Ripple}\tilde{d}_R(s)\right)\right)$$
$$= R(s) - (I + W_{\tau d}\Delta_{\tau d})W_{FA}W_{BEAM}\tilde{d}_B(s) - (I + W_{\tau d}\Delta_{\tau d})WPKC(s)E^k(s)$$
$$-(I + W_{\tau d}\Delta_{\tau d})W_{FA}PW_{Ripple}\tilde{d}_R(s) \quad (I + (I + W_{\tau d}\Delta_{\tau d})W_{FA}PKC(s))E^k(s) = R(s) - (I + W_{\tau d}\Delta_{\tau d})W_{FA}W_{BEAM}\tilde{d}_B(s) - (I + W_{\tau d}\Delta_{\tau d})W_{FA}PW_{Ripple}\tilde{d}_R(s)$$
$$E^k(s) = \left(I + (I + W_{\tau d}\Delta_{\tau d})W_{FA}PKC(s)\right)^{-1}R(s) - \left(I + (I + W_{\tau d}\Delta_{\tau d})W_{FA}PKC(s)\right)^{-1}(I + W_{\tau d}\Delta_{\tau d})W_{FA}W_{BEAM}\tilde{d}_B(s)$$
$$-\left(I + (I + W_{\tau d}\Delta_{\tau d})W_{FA}PKC(s)\right)^{-1}(I + W_{\tau d}\Delta_{\tau d})W_{FA}PW_{Ripple}\tilde{d}_R(s)$$

Hence, the transfer matrix from the exogenous disturbance $\tilde{d}_R$ to error e^k is

$$E^k(s) = -\left(I + (I + W_{\tau d}\Delta_{\tau d})W_{FA}PKC(s)\right)^{-1}(I + W_{\tau d}\Delta_{\tau d})W_{FA}PW_{Ripple}\tilde{d}_R(s)\,. \quad (1)$$

Figure 2 and figure 3 show the frequency responses of the transfer matrix from $\tilde{d}_R$ to error e^k when PI controller I and PI controller II are used, repsectively. Amplitude Ripple is 1.2 % and the Phase Ripple is 11.75 degree. There is a upper limit from the below in the frequency of the HVPS ripple which guarantees the robust performance against the exogenous disturbance, $\tilde{d}_R$, the scaled HVPS ripple. Also, there is a lower limit from the above in the frequency of the HVPS ripple which guarantees the robust performance against the exogenous disturbance, $\tilde{d}_R$, the scaled HVPS ripple. Figure 2 shows that the ripple of the frequency range [5903.9Hz 35966Hz] cannot be rejected with the given PI controller

PI Controller I : $K_P = \begin{bmatrix} 33.2401 & 0.0165 \\ -0.0165 & 33.2401 \end{bmatrix}$, $K_I = 1000e3\begin{bmatrix} 1 & 0 \\ 0 & 1 \end{bmatrix}$

Also, figure 3 shows that the ripple of the frequency range [710.14Hz 30066Hz] cannot be rejected with the given PI controller

PI Controller II : $K_P = \begin{bmatrix} 33.2401 & 0.0165 \\ -0.0165 & 33.2401 \end{bmatrix}$, $K_I = 100e3\begin{bmatrix} 1 & 0 \\ 0 & 1 \end{bmatrix}$

That is, the closed loop systems cannot guarantee the robust performance against the HVPS ripple of the frequency range [5903.9Hz 35966Hz] for PI controller I and [710.14Hz 30066Hz] for PI controller II, respectively.

The given PI controller I and PI controller II are determined so that they do not violate the rule

$$\omega_{BW} \le \omega_C < \frac{1}{\tau d_{\max}}$$

where ω_{BW} is the closed loop system bandwidth which is determined from the transfer matrix from the set point trajectory r to the error e^k (sensitivity matrix), ω_C is the crossover frequency which is determined from the open loop gain matrix, and $\tau d_{\max}$ is the lumped maximum time delay in the whole loop.
The maximum time delay is calculated based on the following time delay data.

$\tau_{Klystron}$ =1.5e-7 sec	: time delay inside the klystron,
τ_{WG} =1.21e-7 sec	: time delay in the waveguide transmission (30ft),
τ_{FBC} =1.21e-7 sec	: time delay in the field signal feedback cable (30ft),
τ_{DSP} =1.0e-6 sec	: time delay for the signal processing in the DSP and interface.

$$\tau d_{\max} = \tau_{Klystron} + \tau_{WG} + \tau_{FBC} + \tau_{DSP} = 1.392 \ \mu \sec .$$

Figure 4 and figure 5 show the frequency responses for the nominal systems, which include the transfer matrix from r to e^k (It is said **Sensitivity Matrix** in the control theory terminology).
In the MATLAB/SIMULINK model simulation, it is shown that when the PI controllers are designed in the way that they violate the rule $\omega_{BW} \le \omega_C < \dfrac{1}{\tau d_{\max}}$, the closed loop system responses shows significant oscillations. The open loop system bandwidth is about 576 Hz (3622 rad/sec). Also, 1/1.392e-006=7.1839e+005 rad/sec. Hence, the controller gain matrix spaces are relative large and so, it is more free to choose PI controller gain matrices K_P and K_I, specially it is less restrictive to determine K_I. Note that, PI conctroller I has $K_I = 1000e3 \cdot I$ and PI controller II has $K_I = 100e3 \cdot I$

Similarly, for other set of amplitude ripple-phase ripple upper limits and lower limits are obtained. Table 1 shows the results which are verified by nonlinear simulations using MATLAB/SIMULINK model of the linear accelerator RF system. Figure 6 shows the upper limit to the high voltage power supply ripple frequency from the below and figure 7 shows the lower limit to the high voltage power supply ripple frequency from the above. The HVPS ripple frequency in the range of [upper limit from the below lower limit from the above] does not guarantee robust performance of the closed loop system with the given PI controller I or PI controller II. Note that, for the cathode ripple which is less than or equal to 825, there are no frequency region that cannot guarantee robust performance with PI controller I or PI controller II.

Remark : Since inside the SRF cavity, there is the cavity field amplitude dependent Lorentz Force Detuning. This Lorentz Force Detuning is the time varying signal whose dynamics is governed by the mechanical time constant 1msec. Hence, in order to attenuate the effect of the Lorentz Force Detuning, the closed loop system has sensitivity matrix profile such that at low frequency, it is as small as possible. Table 1 shows that when only the HVPS ripple is considered, the PI controller I and PI controller II both guarantee required performance for 0.85 % amplitude ripple and 8.5 degree phase ripple. However, due to the Lorentz Force Detuning, PI controller II needs longer time for the field errors are settling down to the required performance specification. In contrast, PI controller I drives the field errors into the required performance specification in a short time (settling time) even though there is time varying Lorentz Force Detuning. Hence, PI controller I is recommended. If the SRF cavity is pretuned against the Lorentz Force Detuning, PI controller II may work for the required performance specification.

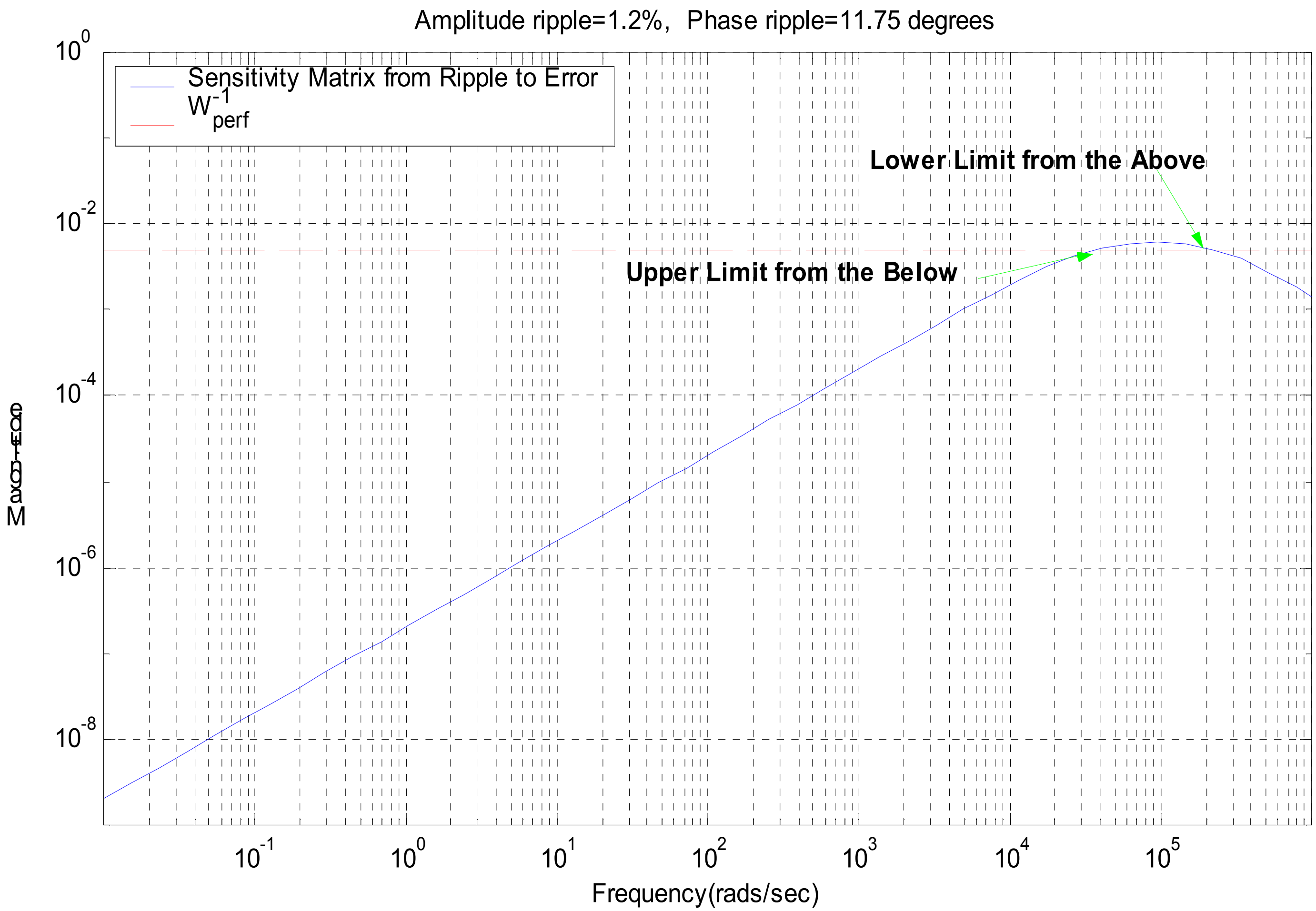

Figure 2 Transfer Matrix from the scaled High Voltage Power Supply (HVPS) ripple to the tracking error when Amplitude Ripple is 1.2 % and the Phase Ripple is 11.75 degree. The PI controller I is used for feedback controller

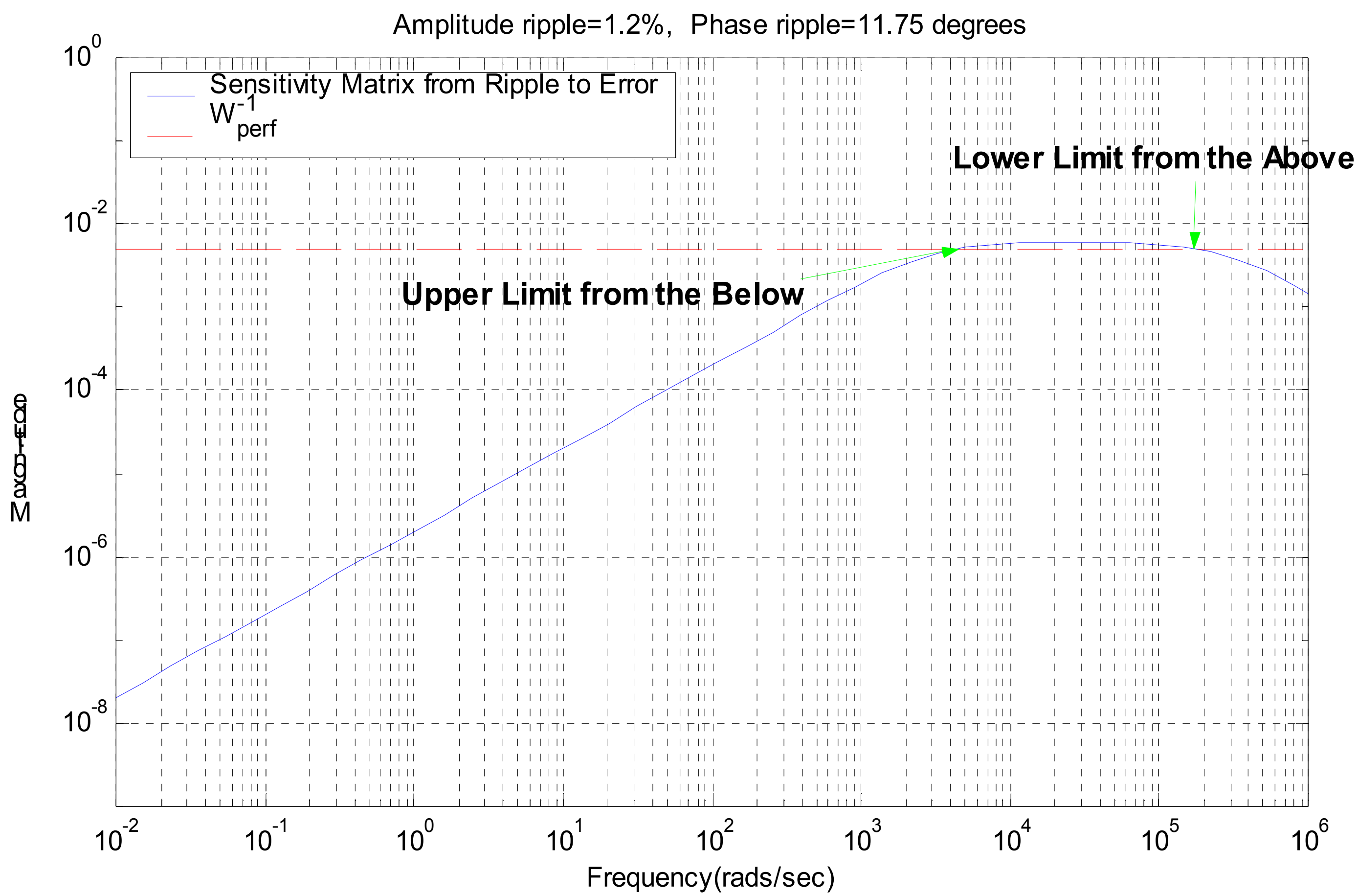

Figure 3 Transfer Matrix from the scaled High Voltage Power Supply (HVPS) ripple to the tracking error when Amplitude Ripple is 1.2 % and the Phase Ripple is 11.75 degree. The PI controller II is used for feedback controller

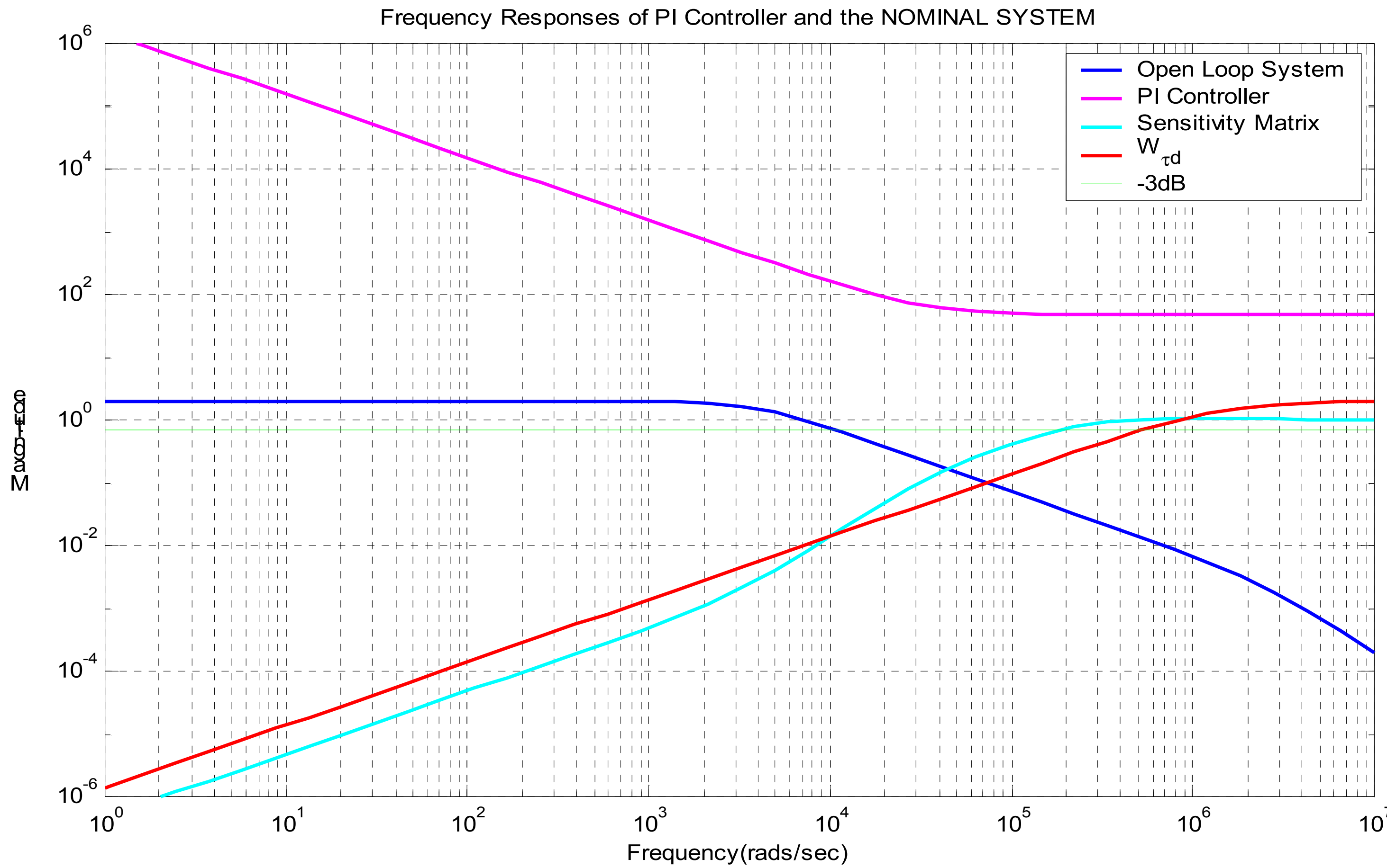

Figure 4 Transfer Matrix (Sensitivity Matrix) from the set point trajectory to the tracking error when Amplitude Ripple is 1.2 % and the Phase Ripple is 11.75 degree. The PI controller I is used for feedback controller

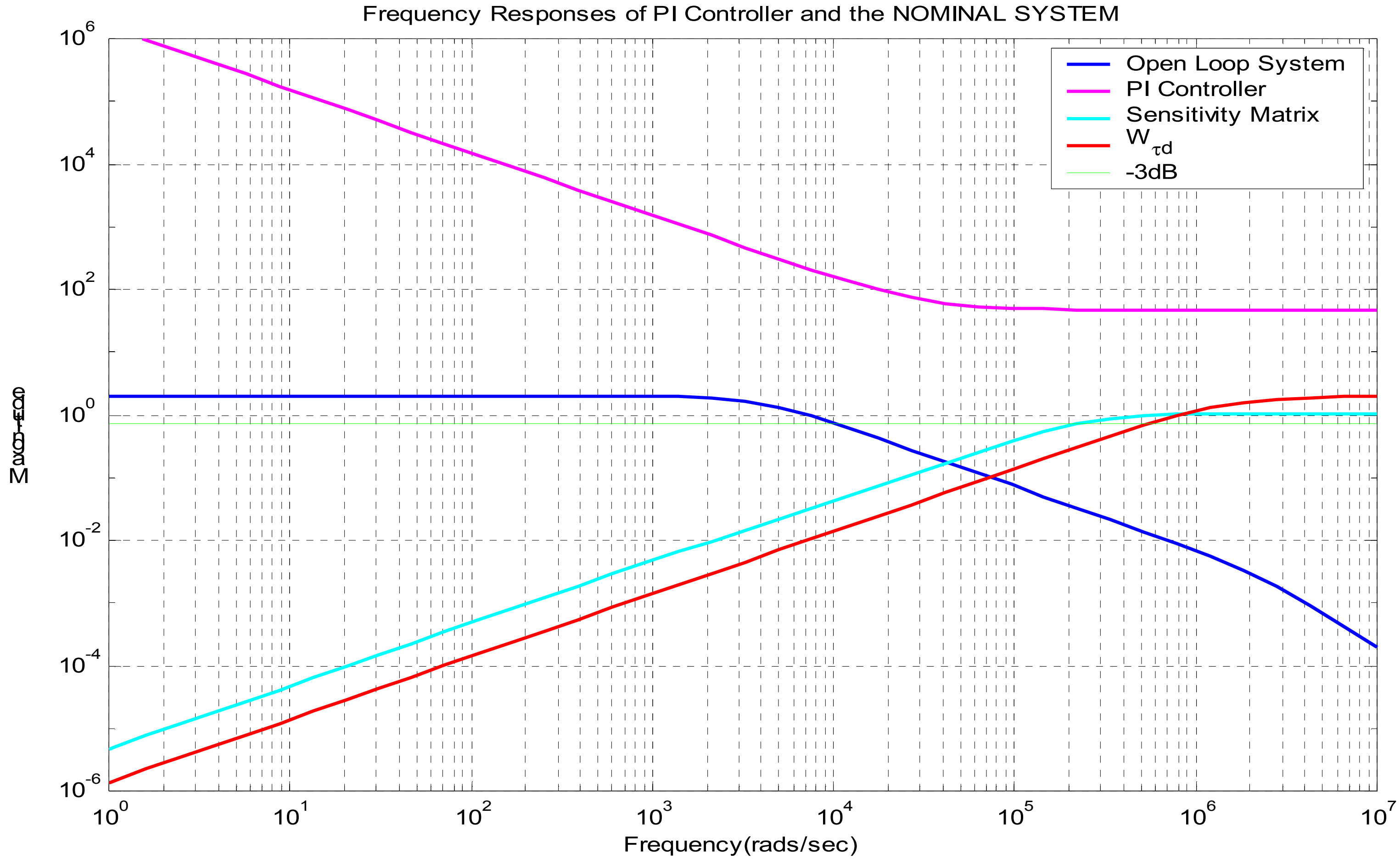

Figure 5 Transfer Matrix (Sensitivity Matrix) from the set point trajectory to the tracking error when Amplitude Ripple is 1.2 % and the Phase Ripple is 11.75 degree. The PI controller II is used for feedback controller

Table 1

Cathode Ripple Voltage (V_{pp})	Amplitude Ripple (%)	Phase Ripple (Degrees)	Frequency Limits for Robust Performance			
			Upper Limit from the Below (Hz)		Lower Limit from the Above (Hz)	
			PI Controller I	PI Controller II	PI Controller I	PI Controller II
250	0.25	2.5	Unlimited	Unlimited	Unlimited	Unlimited
300	0.325	3.1	Unlimited	Unlimited	Unlimited	Unlimited
400	0.425	4.1	Unlimited	Unlimited	Unlimited	Unlimited
500	0.525	5.1	Unlimited	Unlimited	Unlimited	Unlimited
600	0.625	6.7	Unlimited	Unlimited	Unlimited	Unlimited
700	0.75	7.2	Unlimited	Unlimited	Unlimited	Unlimited
825	0.85	8.5	Unlimited	Unlimited	Unlimited	Unlimited
950	1.0	9.75	12977	3183.1	17343	6047.9
1150	1.2	11.75	5903.9	710.14	35966	30066
4000	4.18	36.32	1268.3	128.01	154100	152810

PI Controller I : $K_P = \begin{bmatrix} 33.2401 & 0.0165 \\ -0.0165 & 33.2401 \end{bmatrix}, \quad K_I = 1000e3\begin{bmatrix} 1 & 0 \\ 0 & 1 \end{bmatrix}$

PI Controller II : $K_P = \begin{bmatrix} 33.2401 & 0.0165 \\ -0.0165 & 33.2401 \end{bmatrix}, \quad K_I = 100e3\begin{bmatrix} 1 & 0 \\ 0 & 1 \end{bmatrix}$

Data Sampling Frequency : 20 MHz

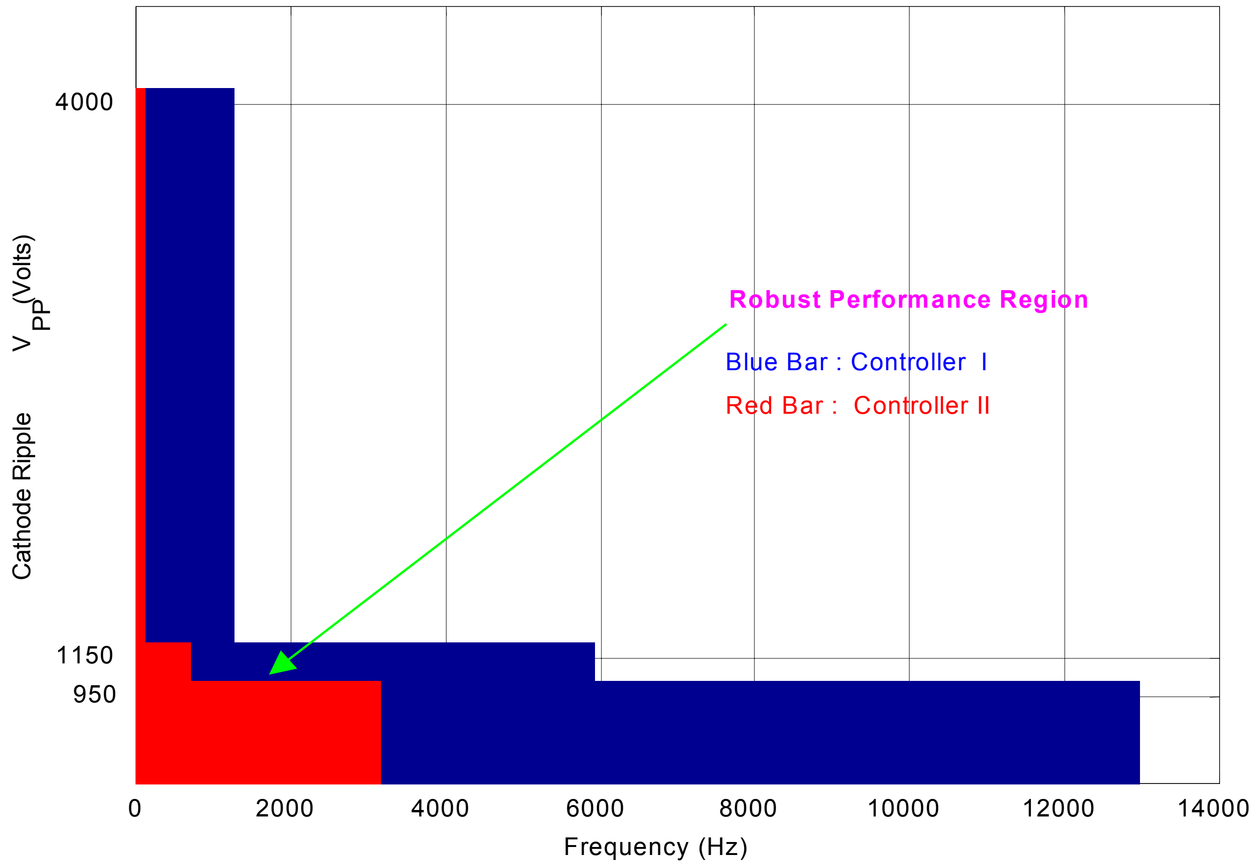

Figure 6 Upper Limit of the HVPS ripple frequency of from the Below

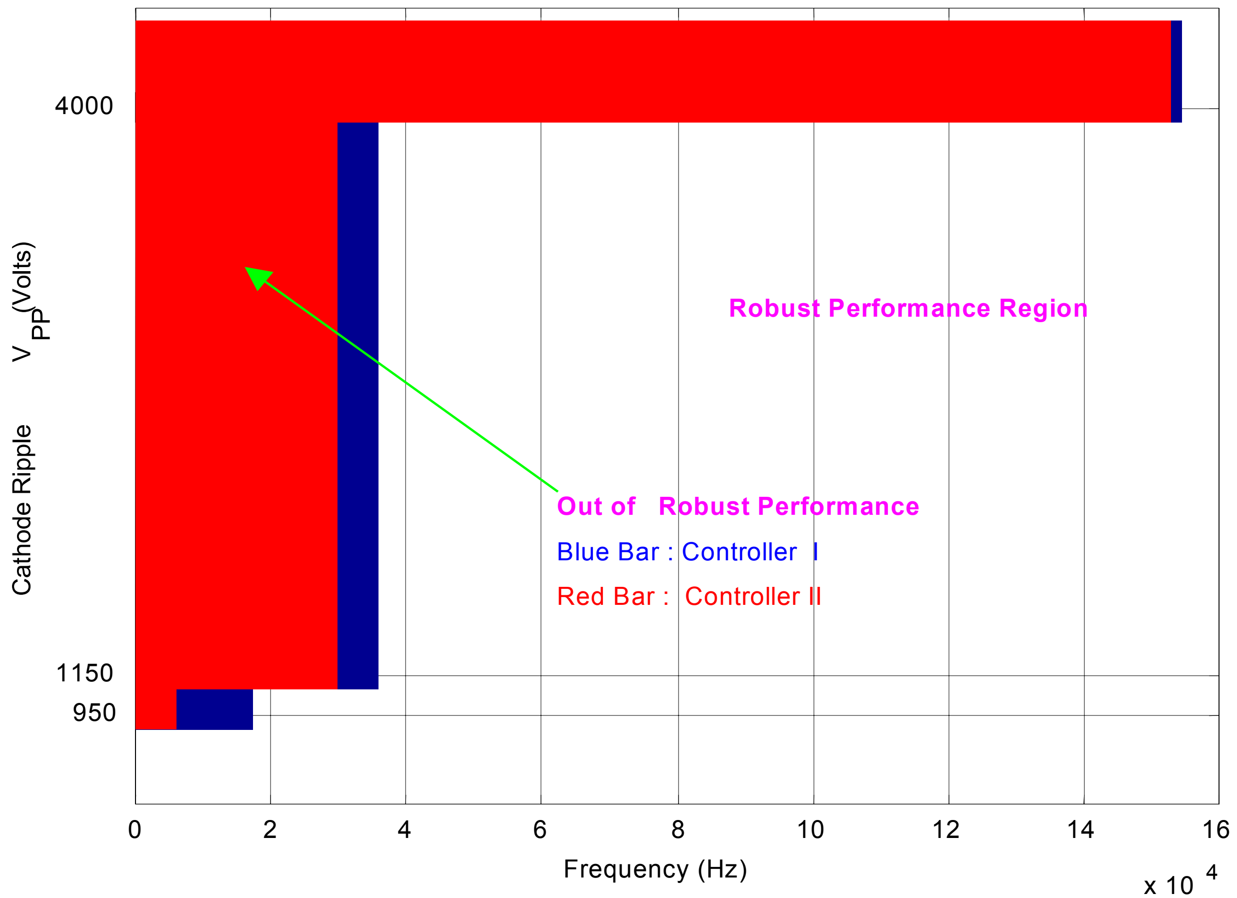

Figure 7 Lower Limit of the HVPS ripple frequency of from the Above

On Figure 8-10:

The ripple frequency is 60 Hz and is a sinusoidal signal with phase so that during the beam on period (flat-top), it can reach its maximum. The amplitude ripple prcentage is 1.2 % and the phase ripple is 11.75 degree. When the ripple is maximal at the end of the beam beriod, the field amplitude error is 0.06 %, and the field phase error is 0.03 degree. However, it is believed that the contributions to these errors are not from the ripple but from other noises, such as the loop noise in the LLRF system of bandwidth of 600 Hz, and the 1.2 % beam noise whose dominant frequency is about 20 kHz. When 1.2 % beam noise of 30 kHz is simulated, we obtain the similar results.

On Figure 11-12:

In order to compare the effect of the ripple to the cavity field for the closed loop system and for the open loop system, figure 11-12 plot the simulation results together. The ripple signal is the same as shown in figure 8 (60 Hz). For the closed loop system response, as mentioned above, the PI feedback controller suppresses the ripple effect on field amplitude and field phase surprisingly. However, for the open loop system, the ripple is in the field amplitude and field phase without being filtered, and actually they are amplified. This can be explained by referring to the open loop system frequency responses (figure 4-figure 5). The open loop system frequency response plots show that the low frequency disturbance is amplified because the singular values at low frequency is larger than 0 dB(gain =1). For the case of closed loop system, the effect of the disturbance (in this simulation, the ripple) is governed by the sensitivity matrices obtained from (1). Figure 2 and figure 3 show that at the frequency 60 Hz, the magnitudes of the sensitivity matrices are less than –100 dB (gain: 1.08e-005) in figure 2 and –75 dB (gain: 1.8e-005) in figure 3. From the equation (1), the effect of the ripple is not shown in the field amplitude and field phase.

On Figure 13:

In order to understand the compensation of the phase ripple by the PI controller, figure 13 illustrates the phase relations among, Low Level RF phase (controller output phase), phase ripple (36.32 degree), and the normalized ripple signal of 1.0 kHz. Figure 13 shows that the LLRF phase (LLRF PHS) is out of phase (180 degree phase) with respect to the additive phase ripple even though the magnitude is different. As a result, the phase ripple is compensated in the cavity field phase. (Cavity field phase is not plotted but it follows the desired phase, zero degree). Similar results has been shown for the amplitude.

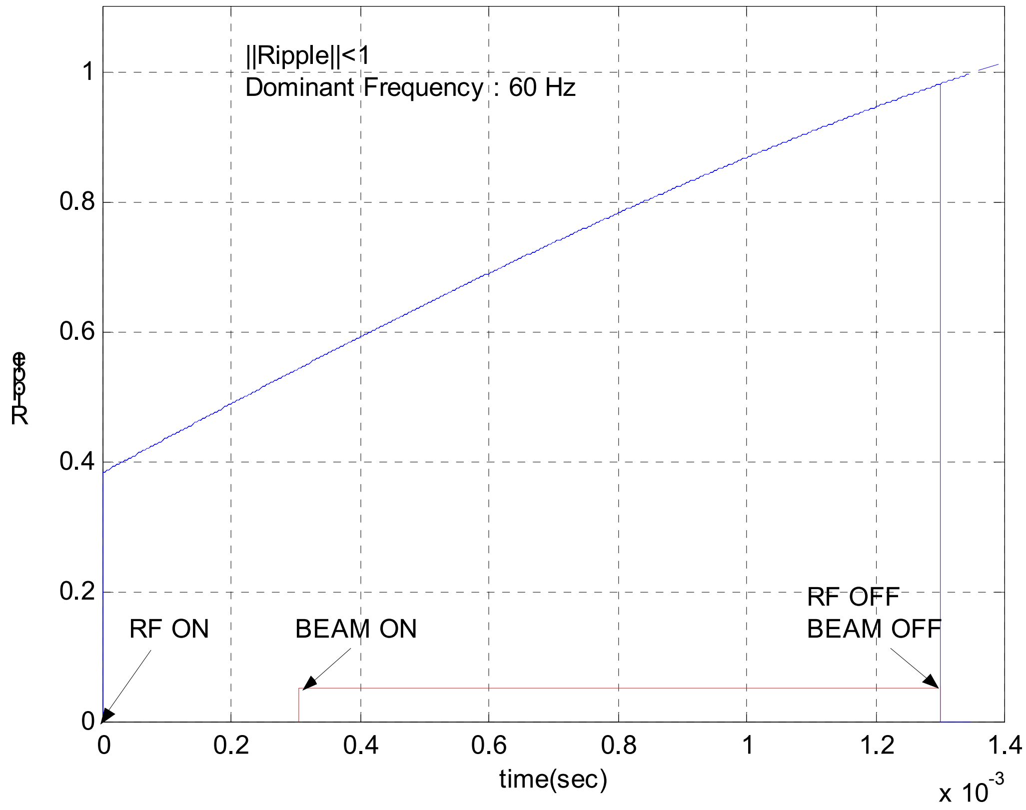

Figure 8 60 Hz ripple

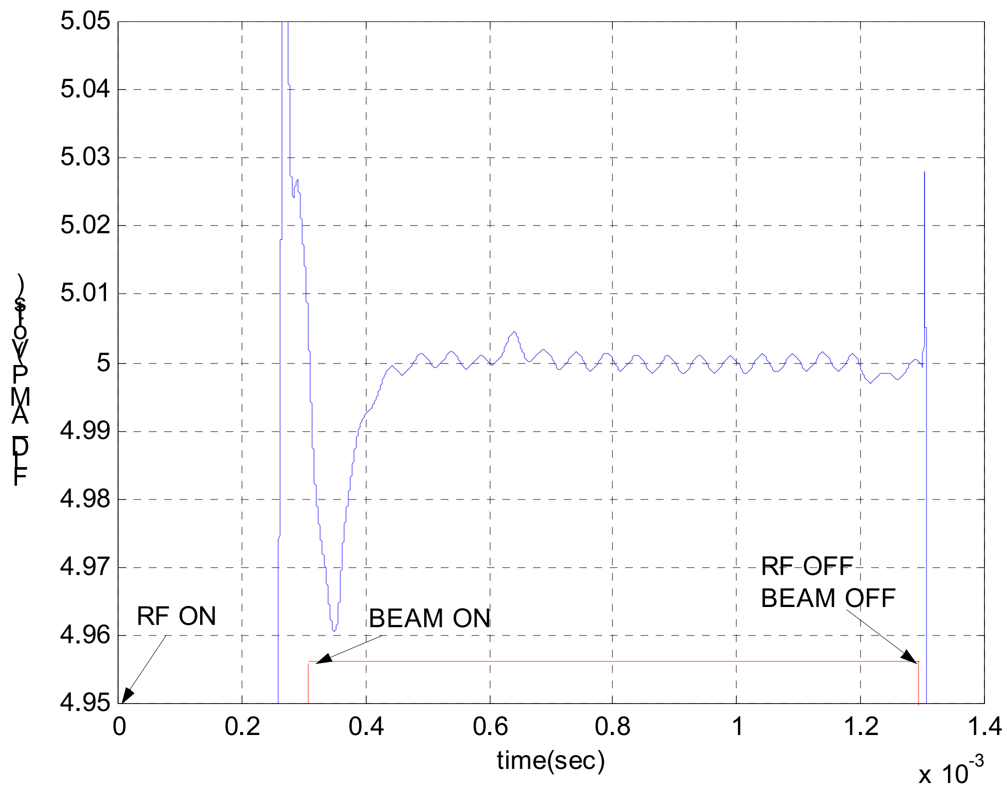

Figure 9 Closed loop. PI controller I is used

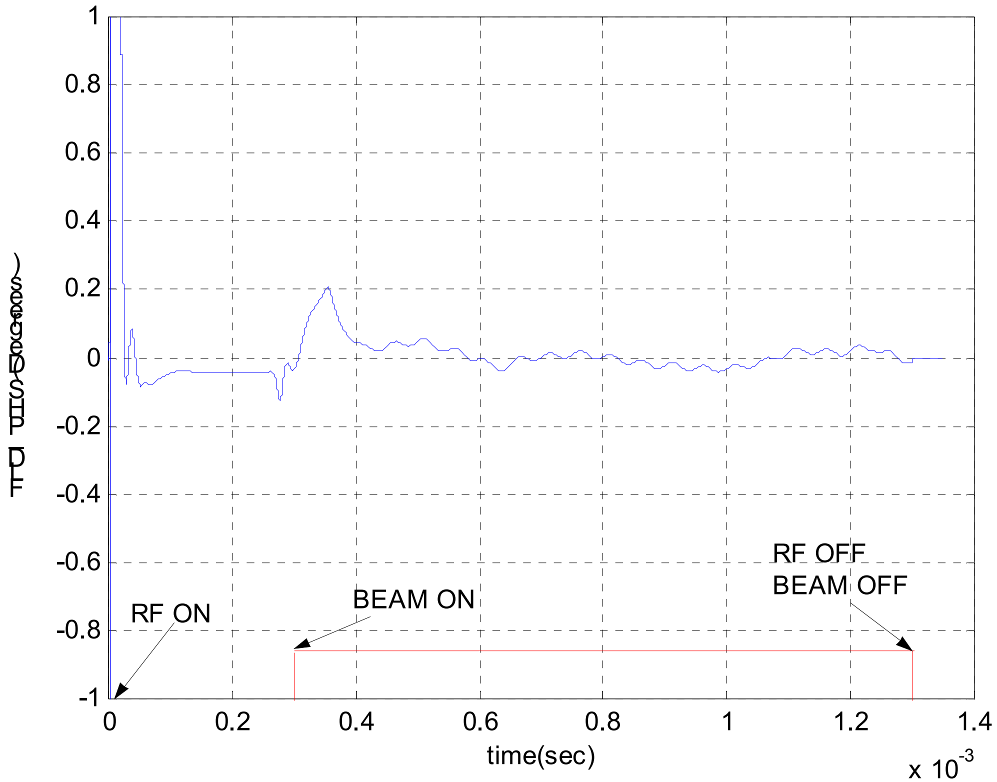

Figure 10 Closed loop system. PI controller I is used

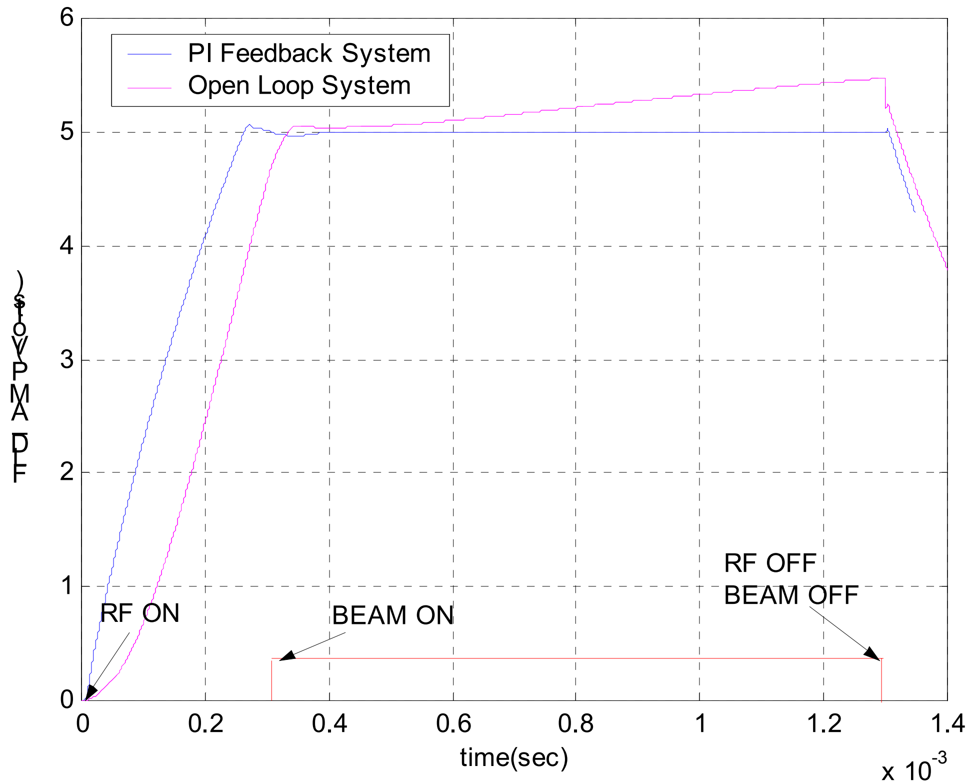

Figure 11 Open Loop and closed loop system comparison for field amplitude

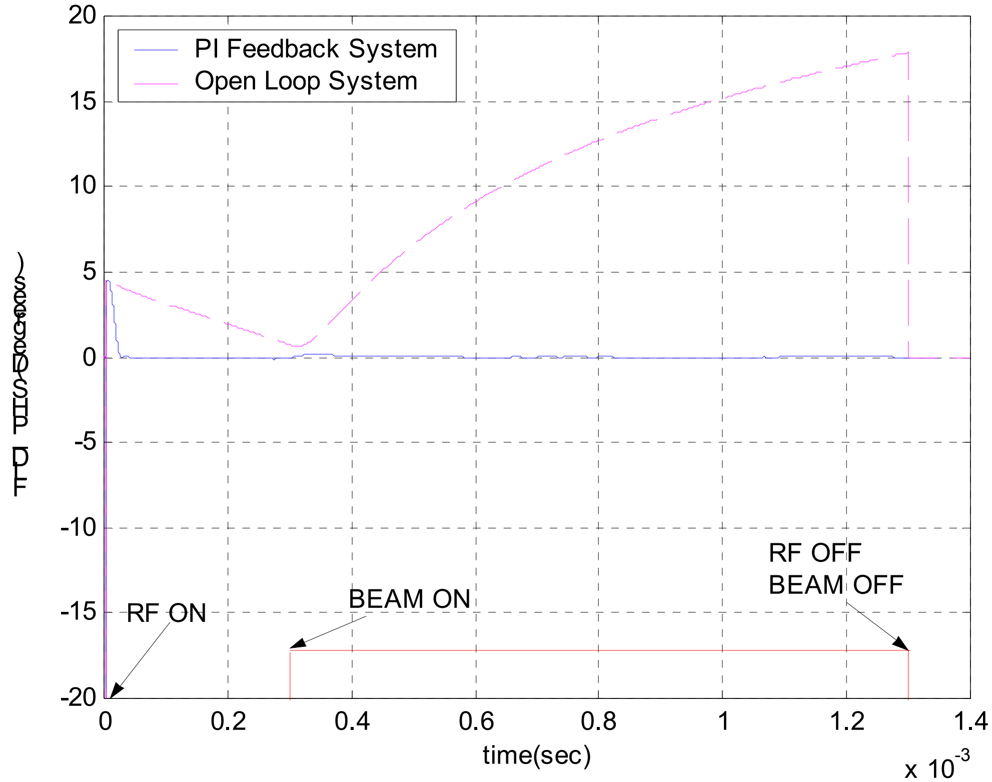

Figure 12 Open Loop and closed loop system comparison for field phase

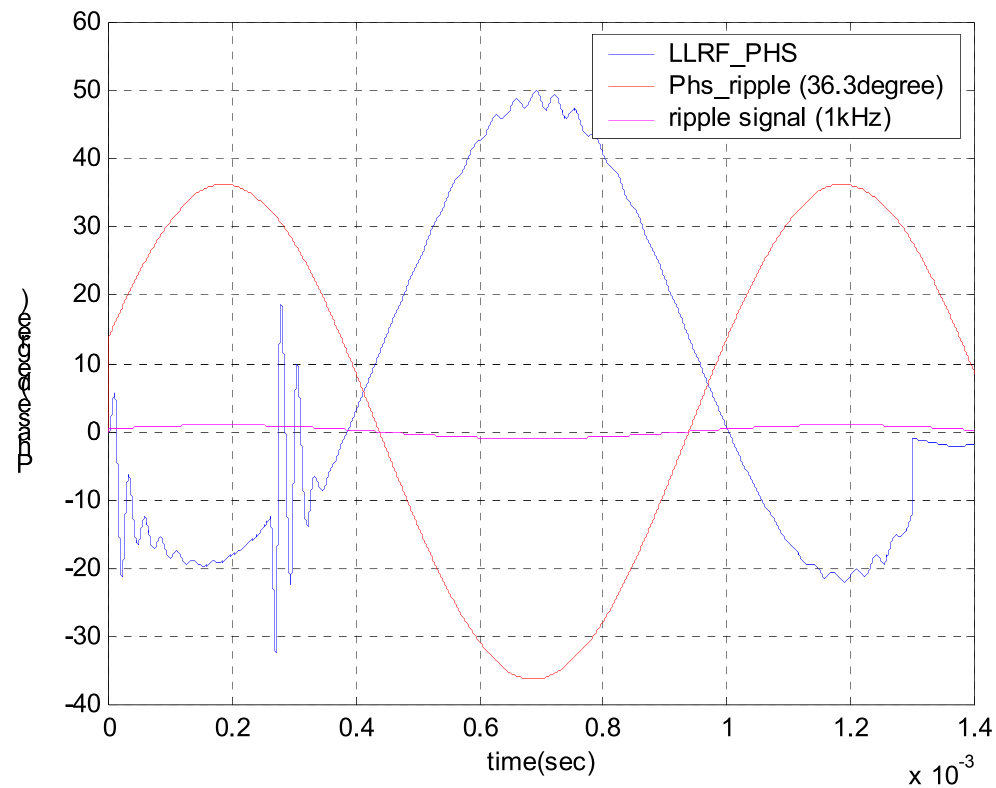

Figure 13 Phases of the controller output signal and phase ripple

3. Sensitivity Matrix for the High Voltage Power Supply Ripple in the Perturbed Closed Loop System of a DTL Tank

The transfer matrix from the exogenous disturbance $\tilde{d}_R$ to error e^k as given by (1) is applied to analyze the effect of the high voltage power supply ripple to the set point tracking error e^k.

Figure 14 shows the frequency response of the transfer matrix from $\tilde{d}_R$ to error e^k.
As is the case of SRF cavity, there is a upper limit from the below in the frequency of the HVPS ripple which guarantees the robust performance against the exogenous disturbance, $\tilde{d}_R$, the scaled HVPS ripple. Also, there is a lower limit from the above in the frequency of the HVPS ripple which guarantees the robust performance against the exogenous disturbance, $\tilde{d}_R$, the scaled HVPS ripple. The plot shows that the ripple of the frequency range [3979 Hz, 440 kHz] can not be rejected with the given PI controller

$$K_P = \begin{bmatrix} 5.0 & 0 \\ 0 & 5.0 \end{bmatrix}, \quad K_I = 1000e3 \cdot \begin{bmatrix} 1 & 0 \\ 0 & 1 \end{bmatrix}.$$

That is, the closed loop system cannot guarantee the robust performance against the HVPS ripple of the frequency range [3979 Hz, 440 kHz].
The given PI controller is determined so that it does not violate the rule

$$\omega_{BW} \le \omega_C < \frac{1}{\tau d_{\max}}$$

where ω_{BW} is the closed loop system bandwidth which is determined from the sensitivity matrix, ω_C is the crossover frequency which is determined from the open loop gain matrix, and $\tau d_{\max}$ is the lumped maximum time delay in the whole loop.

$$\tau d_{\max} = \tau_{Klystron} + \tau_{WG} + \tau_{FBC} + \tau_{DSP} = 1.392 \ \mu\sec .$$

Figure 15 shows the frequency responses for the nominal system, which include the transfer matrix from r to e^k (It is said **Sensitivity Matrix** in the control theory terminology). The open loop system bandwidth is about 15.92 kHz (1.0e+005 rad/sec). Also, $\frac{1}{\tau d_{\max}}$=1/1.392e-006=7.1839e+005 rad/sec. Hence, the controller gain matrix spaces are relative large and so, it is more free to choose PI controller gain matrices K_P and K_I, specially it is less restrictive to determine K_I.

Similarly, for other set of amplitude ripple-phase ripple upper limits and lower limits are obtained. Table 2 shows the results which are verified by nonlinear simulations using MATLAB/SIMULINK model of the linear accelerator RF system. Figure 16 shows the upper limit to the high voltage power supply ripple frequency from the below and figure 17 shows the lower limit to the high voltage power supply ripple frequency from the above. The HVPS ripple frequency in the range of [upper limit from the below lower limit from the above] does not guarantee robust performance of the closed loop system with the given PI controller.

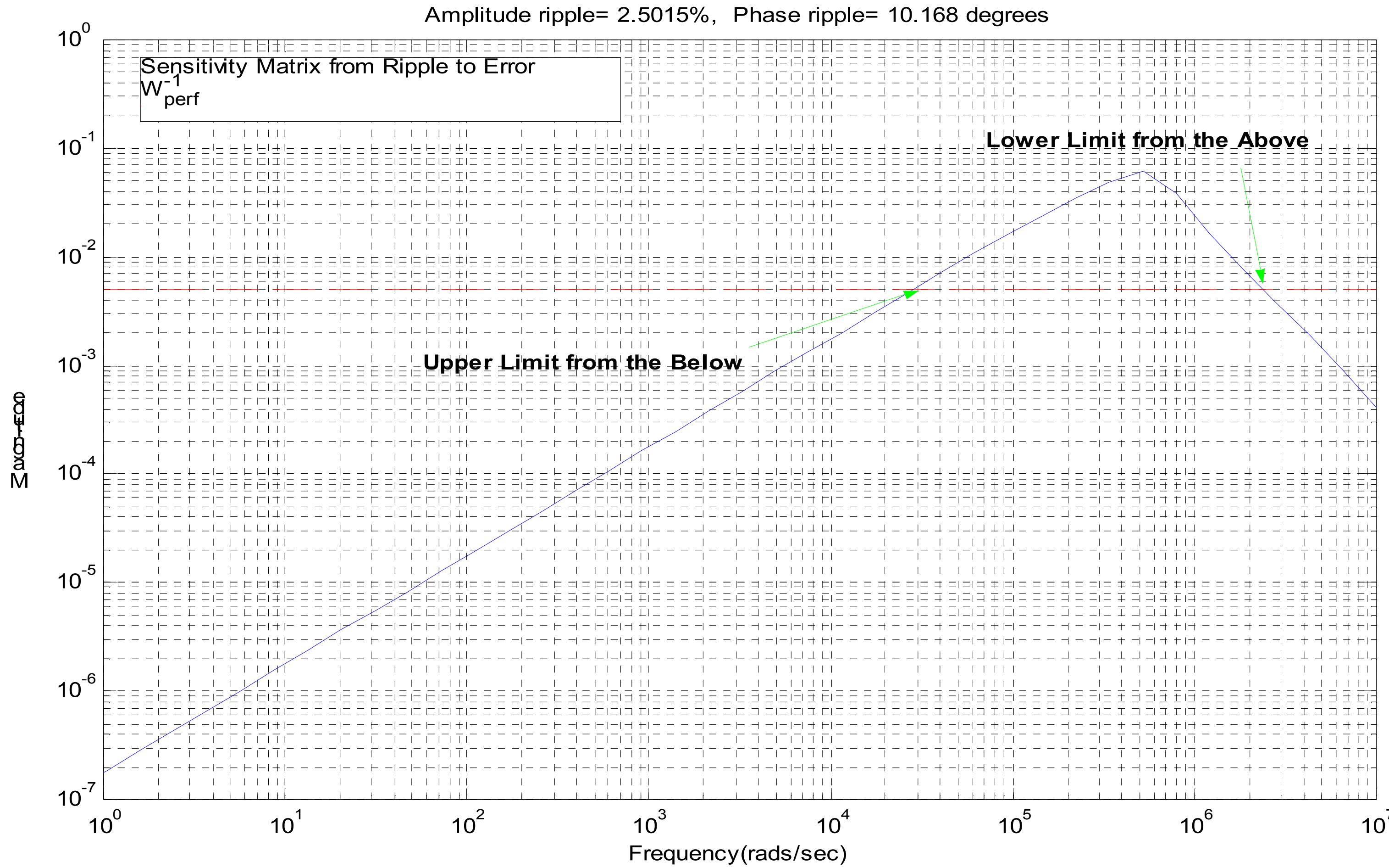

Figure 14 Transfer Matrix from the scaled High Voltage Power Supply (HVPS) ripple to the tracking error when Amplitude Ripple is 2.5015% and the Phase Ripple is 10.168 degree

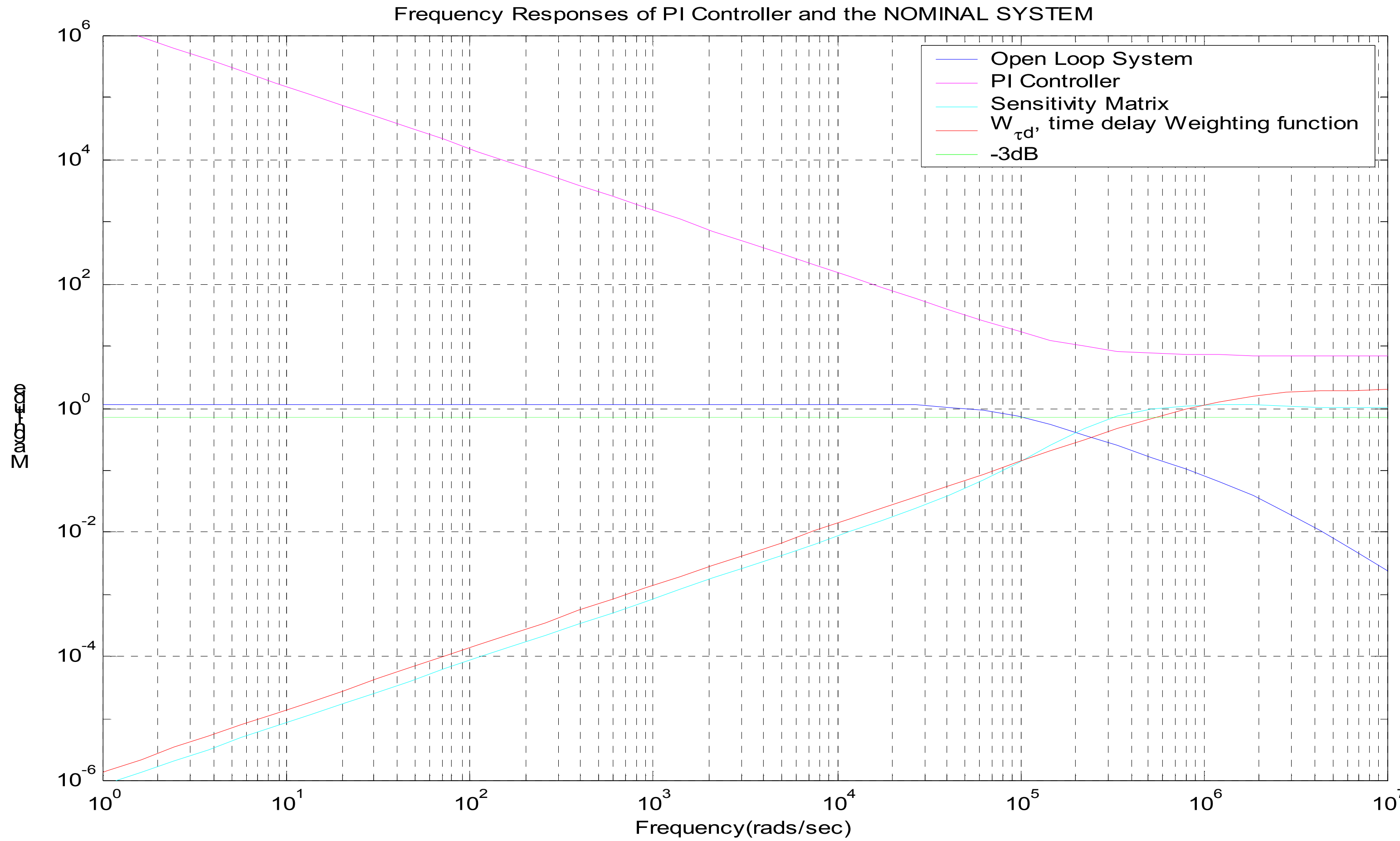

Figure 15 Sensitivity Matrix from the set point trajectory to the tracking error when Amplitude Ripple is 2.5015% and the Phase Ripple is 10.168 degree

Table 2

Cathode Ripple Voltage (V_{pp})	Amplitude Ripple (%)	Phase Ripple (Degrees)	Frequency Limits for Robust Performance	
			Upper Limit from the Below (Hz)	Lower Limit from the Above (Hz)
250	0.141	0.571	Unlimited	Unlimited
300	0.169	0.686	Unlimited	Unlimited
400	0.225	0.914	70577	92732
500	0.281	1.143	49578	1.1324e+005
600	0.337	1.371	39731	1.2756e+005
700	0.394	1.600	32950	1.4395e+005
820	0.461	1.874	27408	1.5832e+005
950	0.534	2.171	23003	1.698e+005
1150	0.647	2.628	18674	1.8238e+005
1780	1.00068	4.067	11666	2.3595e+005
2670	1.50100	6.101	7638.3	2.8516e+005
3570	2.00691	8.157	5655.6	3.5468e+005
4450	2.50154	10.168	4503.8	4.0974e+005

,

PI Controller : $K_P = \begin{bmatrix} 5.0 & 0 \\ 0 & 5.0 \end{bmatrix}$, $K_I = \begin{bmatrix} 1000000 & 0 \\ 0 & 1000000 \end{bmatrix}$

Data Sampling Frequency : 20 MHz

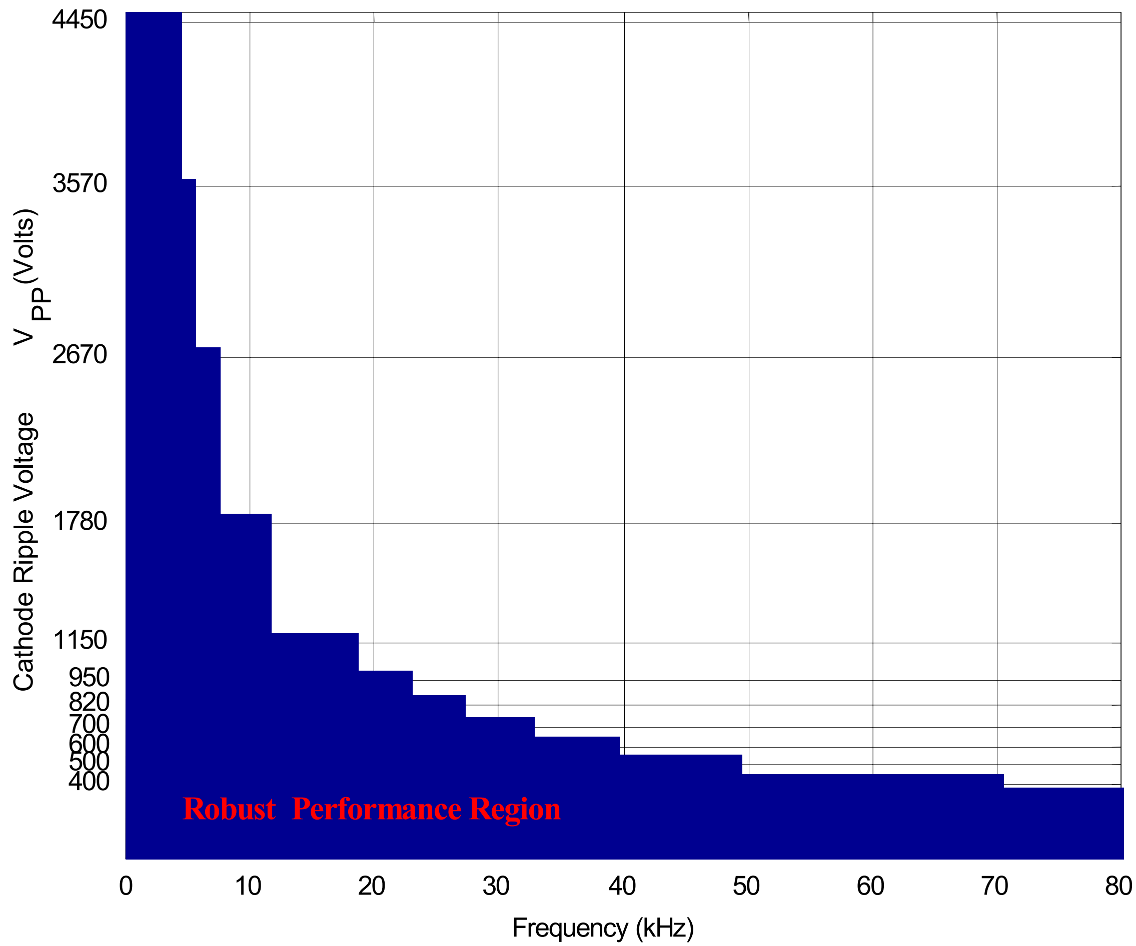

Figure 16 Upper Limit of the HVPS ripple frequency of from the Below

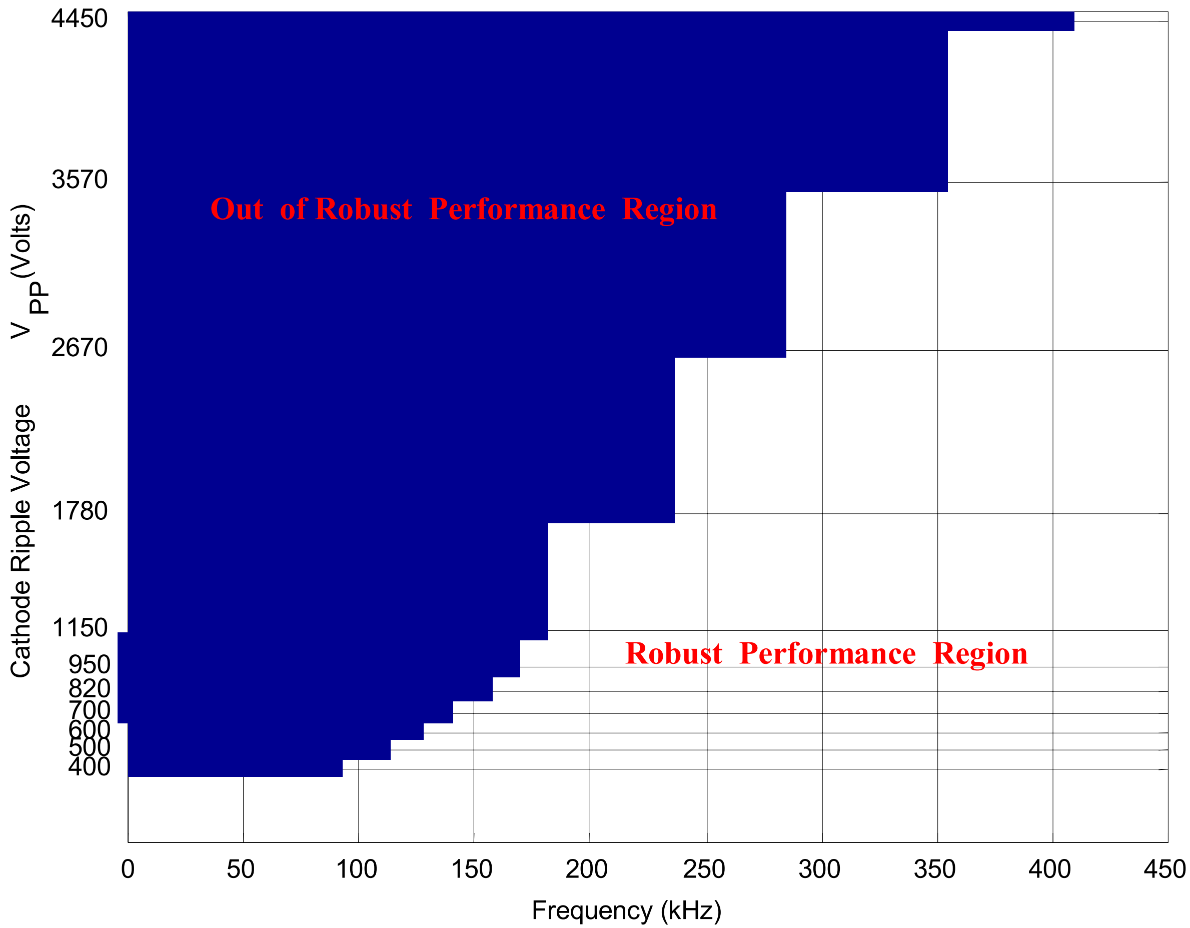

Figure 17 Lower Limit of the HVPS ripple frequency of from the Above

4. Sensitivity Matrix for the High Voltage Power Supply Ripple in the Perturbed Closed Loop System of a DTL Tank

The transfer matrix from the exogenous disturbance $\tilde{d}_R$ to error e^k as given by (1) is applied to analyze the effect of the high voltage power supply ripple to the set point tracking error e^k.

Figure 18 shows the frequency response of the transfer matrix from $\tilde{d}_R$ to error e^k.
There is a upper limit from the below in the frequency of the HVPS ripple which guarantees the robust performance against the exogenous disturbance, $\tilde{d}_R$, the scaled HVPS ripple. Also, there is a lower limit from the above in the frequency of the HVPS ripple which guarantees the robust performance against the exogenous disturbance, $\tilde{d}_R$, the scaled HVPS ripple. The plot shows that the ripple in the frequency range [3979 Hz, 440 kHz] can not be rejected with the given PI controller

$$K_P = \begin{bmatrix} 1.5 & 0 \\ 0 & 1.5 \end{bmatrix}, \qquad K_I = \begin{bmatrix} 525000 & 0 \\ 0 & 525000 \end{bmatrix}.$$

The given PI controller is determined so that it does not violate the rule

$$\omega_{BW} \le \omega_C < \frac{1}{\tau d_{\max}}.$$

The maximum time delay is

$$\tau d_{\max} = \tau_{Klystron} + \tau_{WG} + \tau_{FBC} + \tau_{DSP} = 1.392 \ \mu \sec .$$

Figure 19 shows the frequency responses for the nominal system, which include the transfer matrix from r to e^k (It is said **Sensitivity Matrix** in the control theory terminology). The open loop system bandwidth is about 63.7 kHz (400e3 rad/sec). Also, $\frac{1}{\tau d_{\max}}$=1/1.392e-006=718.39e+003 rad/sec. Hence, the controller gain matrix spaces are not large. Specially, the determination of the integrator gain matrix K_I is stringent. For other set of amplitude ripple-phase ripple, upper limits and lower limits are obtained. Table 3 shows the results which are verified by nonlinear simulations using

MATLAB/SIMULINK model of the linear accelerator RF system. Figure 20 shows the upper limit to the high voltage power supply ripple frequency from the below and figure 21 shows the lower limit to the high voltage power supply ripple frequency from the above. The HVPS ripple frequency in the range of [upper limit from the below lower limit from the above] does not guarantee robust performance of the closed loop system with the given PI controller. Figure 22 shows the upper limit comparison for the DTL Tank #3 and CCL module #4.

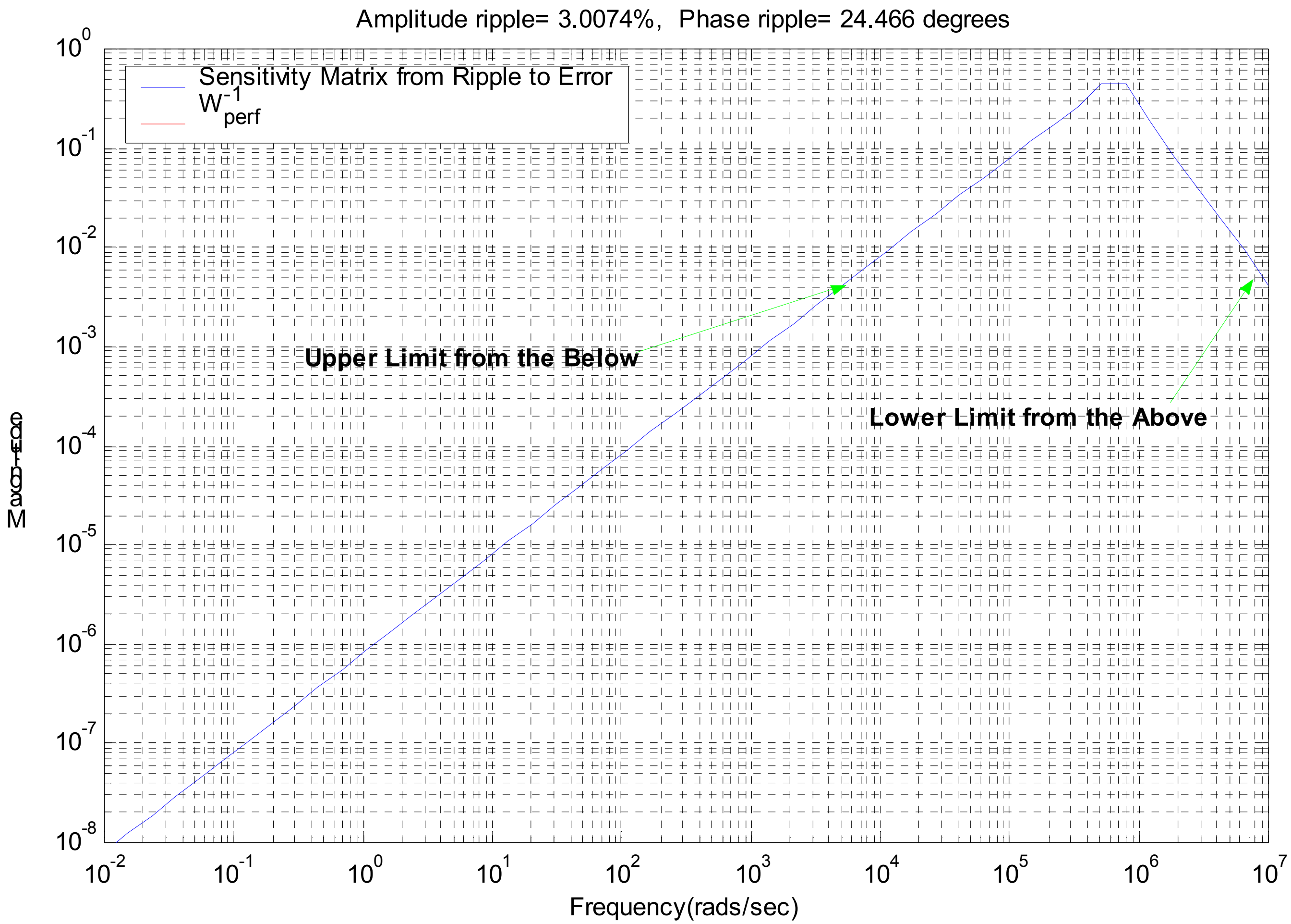

Figure 18 Transfer Matrix from the scaled High Voltage Power Supply (HVPS) ripple to the tracking error when Amplitude Is 3.00737 % and the phase Ripple is 24.46555 degree

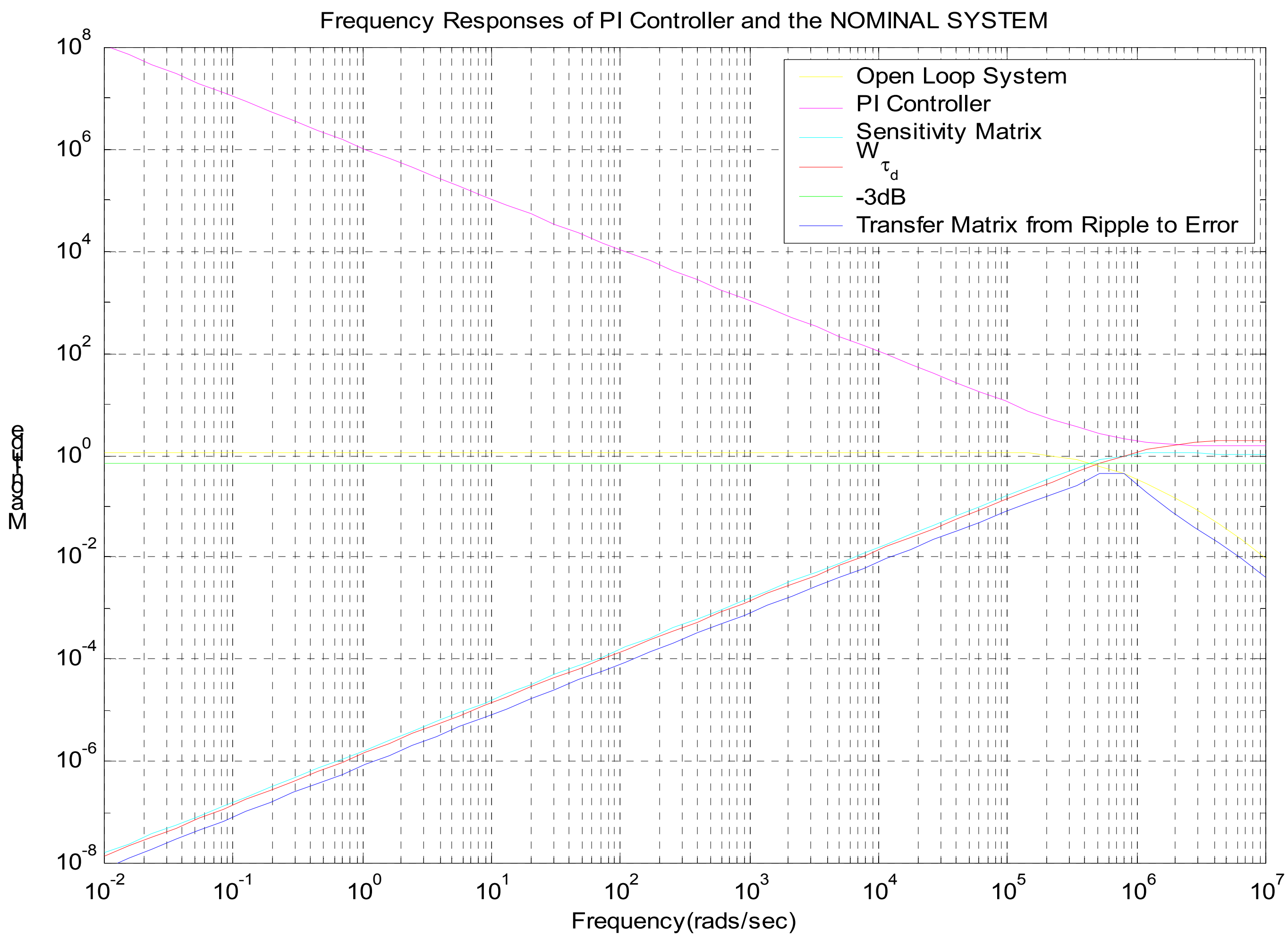

Figure 19 Sensitivity Matrix from the set point trajectory to the tracking error when Amplitude Ripple is 3.00737 % and the phase Ripple is 24.46555 degree

Table 3

Cathode Ripple Voltage (V_{pp})	Amplitude Ripple (%)	Phase Ripple (Degrees)	Frequency Limits for Robust Performance	
			Upper Limit from the Below (Hz)	Lower Limit from the Above (Hz)
250	0.141	1.143	22113	2.6603e+005
300	0.169	1.372	18300	2.8358e+005
400	0.225	1.829	13593	3.4023e+005
500	0.281	2.287	10819	3.9526e+005
600	0.337	2.744	8989.4	4.3478e+005
700	0.394	3.201	7692.3	4.8646e+005
825	0.464	3.773	6511	5.5107e+005
950	0.534	4.344	5648.4	5.9850e+005
1150	0.647	5.259	4656.9	6.5309e+005
1780	1.00068	8.09421	3012	8.6084e+005
2675	1.50381	12.23278	1981.5	1.0275e+006
3575	2.00972	16.34848	1474.7	1.2582e+006
4450	2.50154	20.34985	1178.6	1.4127e+006
5400	3.00737	24.46555	975.17	1.5189e+006

,

PI Controller : $K_P = \begin{bmatrix} 1.5 & 0 \\ 0 & 1.5 \end{bmatrix}$, $K_I = \begin{bmatrix} 525000 & 0 \\ 0 & 525000 \end{bmatrix}$

Data Sampling Frequency : 20 MHz

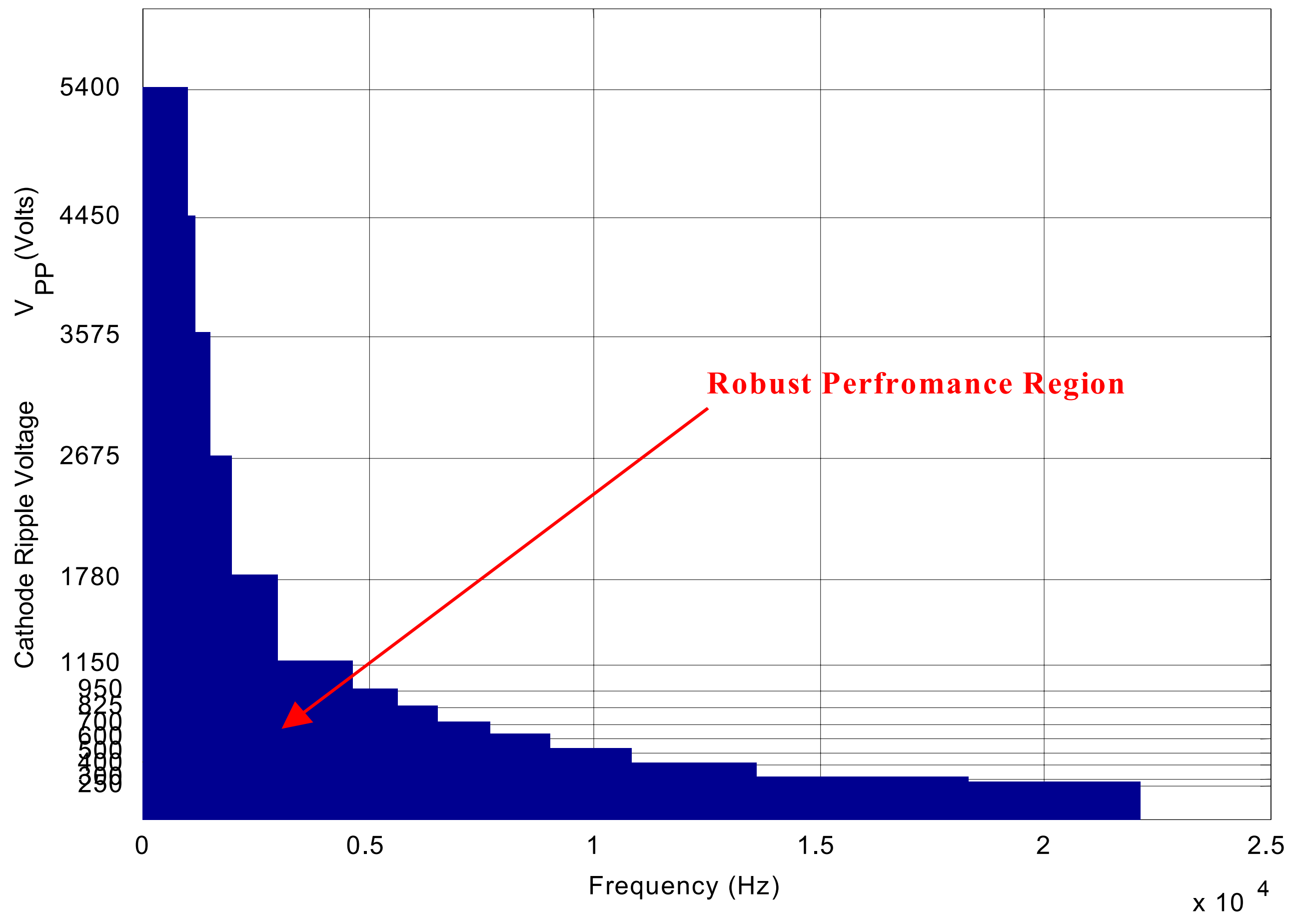

Figure 20 Upper Limit of the HVPS ripple frequency of from the Below

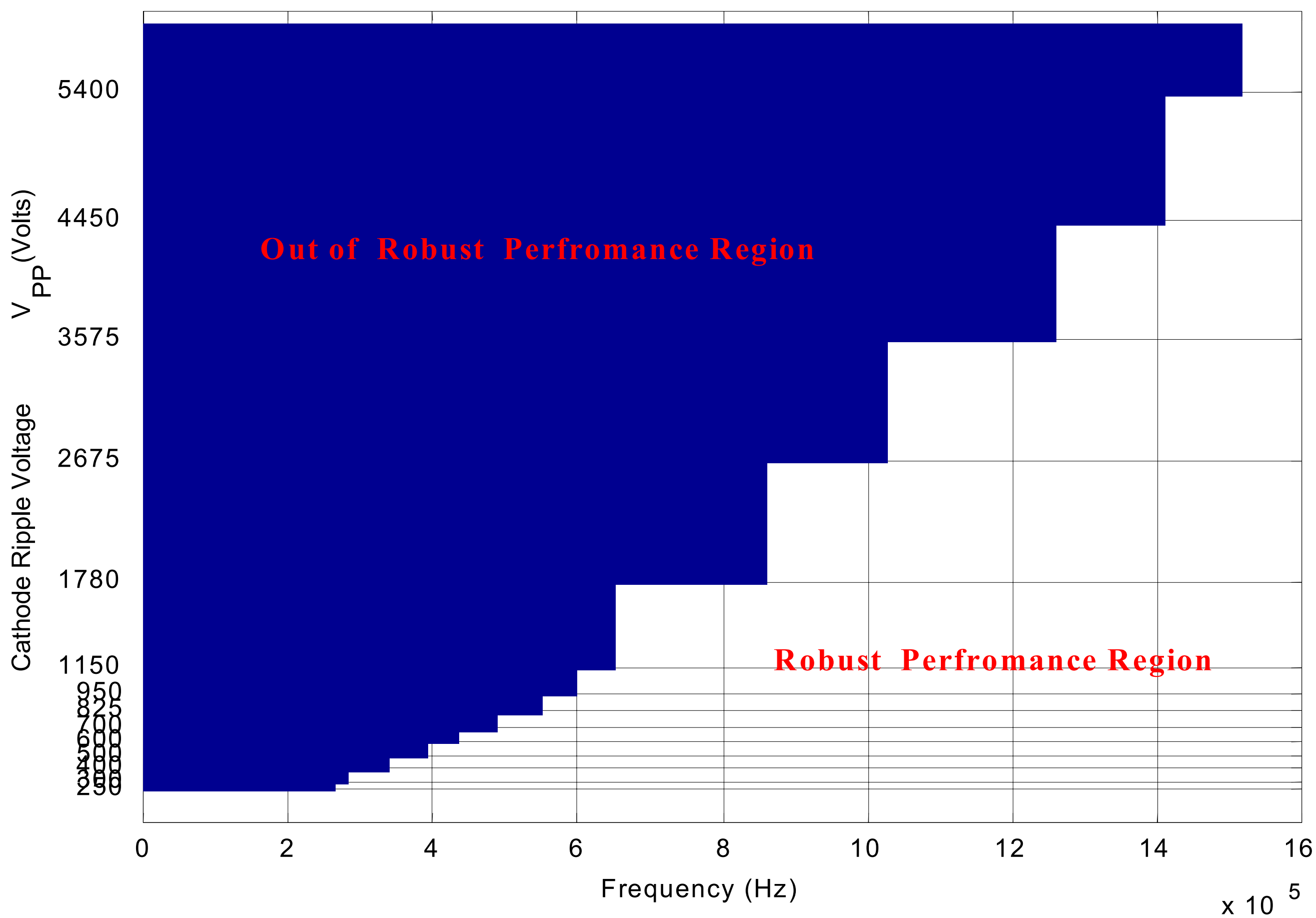

Figure 21 Lower Limit of the HVPS ripple frequency of from the Above

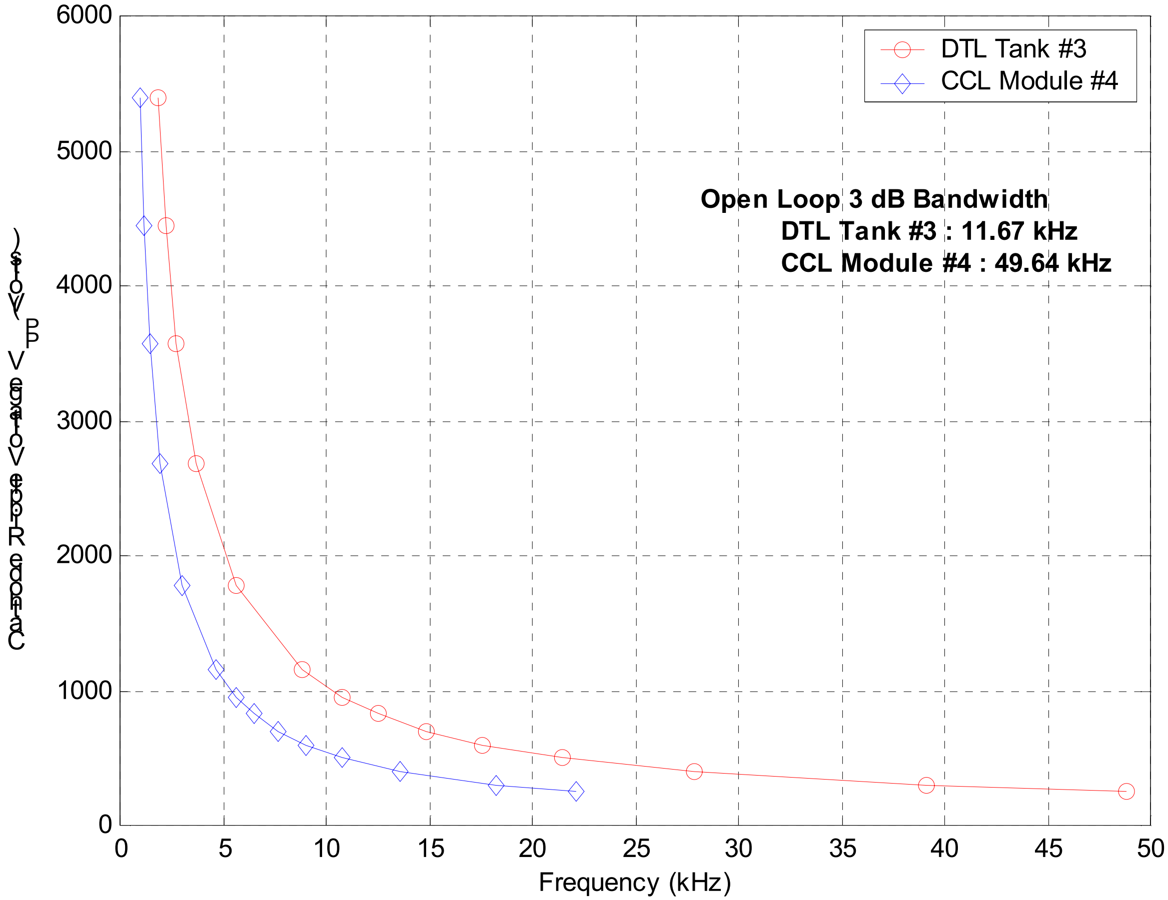

Figure 22 Comparison of Upper Limits of the HVPS ripple frequency of from the Below